Electronic Supplementary Material (ESI) for Journal of Materials Chemistry A.
This journal is © The Royal Society of Chemistry 2021

Supplementary Information

Natural forest-inspired Ag lithiophilic porous arrays grown in the Cu foam hosts with bi-continuous electronic/ionic pathways for highly stable Li metal anodes

Lulu Wu, Weiwei Jiang, Hantao Zou, Chengzhou Ye, Jing Zhang, Guojun Xu, Xiaomin Li, Zhihao Yue, Fugen Sun*, Lang Zhou

Institute of Photovoltaics, Nanchang University, 999 Xuefu Road, Nanchang, 330031, China

Corresponding author：Fugen Sun

E-mail : sunfugen@ncu.edu.cn

Address: *Institute of Photovoltaics, Nanchang University, 999 Xuefu Road, Nanchang, 330031, China*

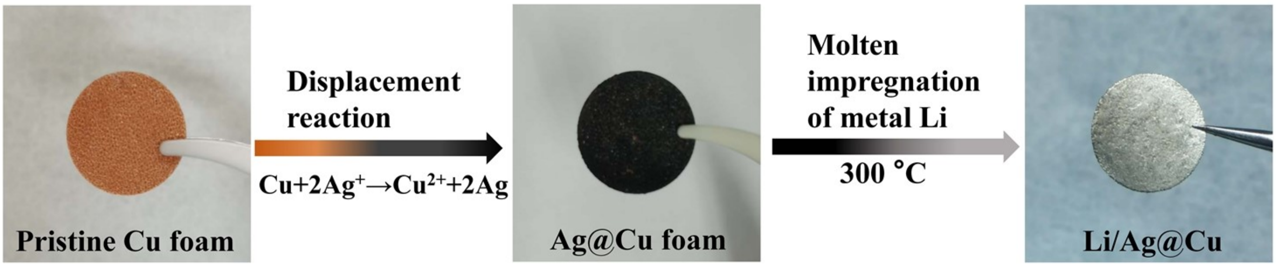

Fig. S1. Photographs of the pristine Cu, Ag@Cu foams and Li/Ag@Cu composites.

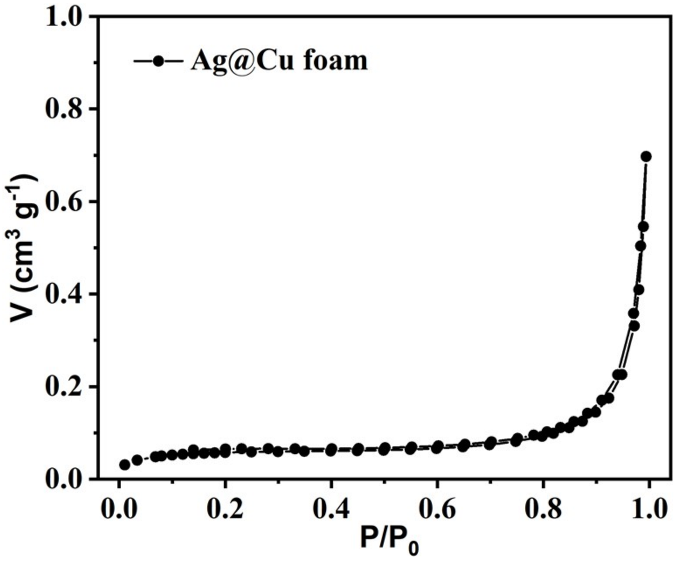

Fig. S2. N_2 adsorption-desorption isotherms of the Ag@Cu foams.

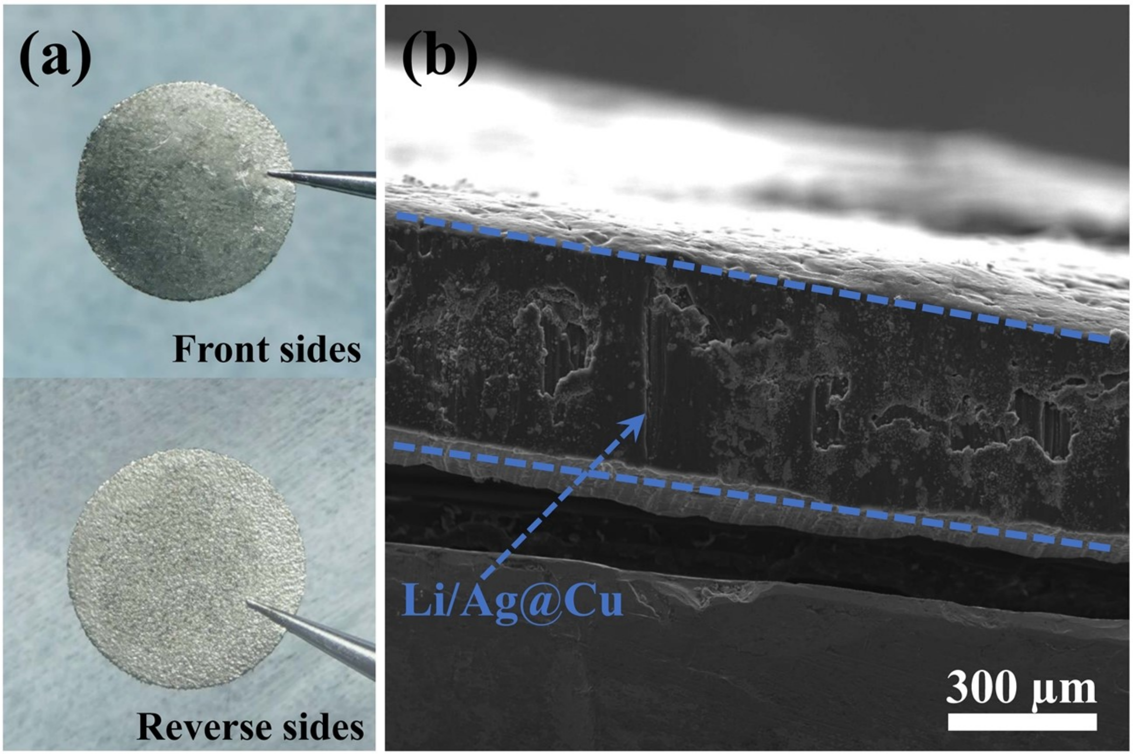

Fig. S3. (a) Photographs of different sides of the Li/Ag@Cu sheets and (b) the SEM image of the cross-section side of the cut Li/Ag@Cu sheets.

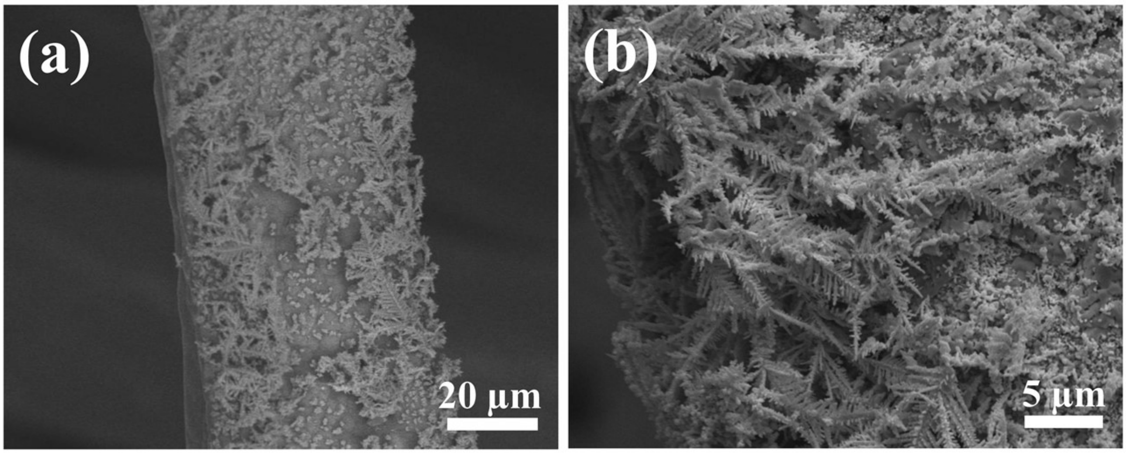

Fig. S4. (a-b) SEM image of the Li/Ag@Cu anodes after fully stripping of metal Li.

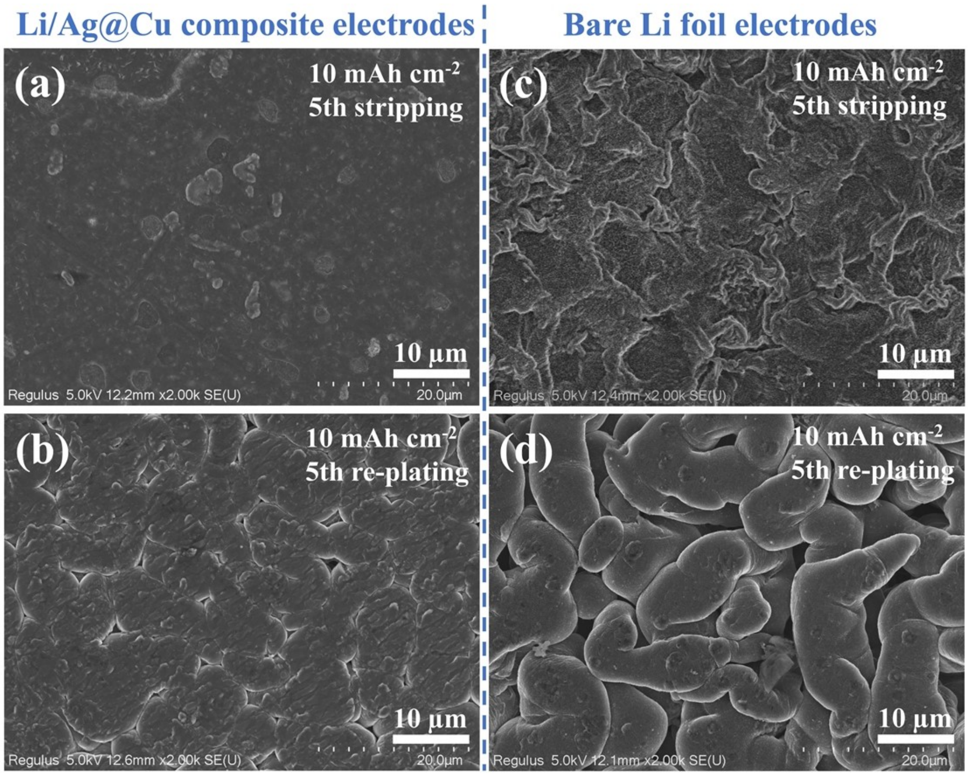

Fig. S5. SEM images of the Li/Ag@Cu composite electrodes after (a) 5th Li stripping and (b) 5th Li re-plating with a capacity of 10 mAh cm^{-2} at a current density of 5 mA cm^{-2}. SEM images of the bare Li electrodes after (c) 5th Li stripping and (d) 5th Li re-plating with a capacity of 10 mAh cm^{-2} at a current density of 5 mA cm^{-2}.

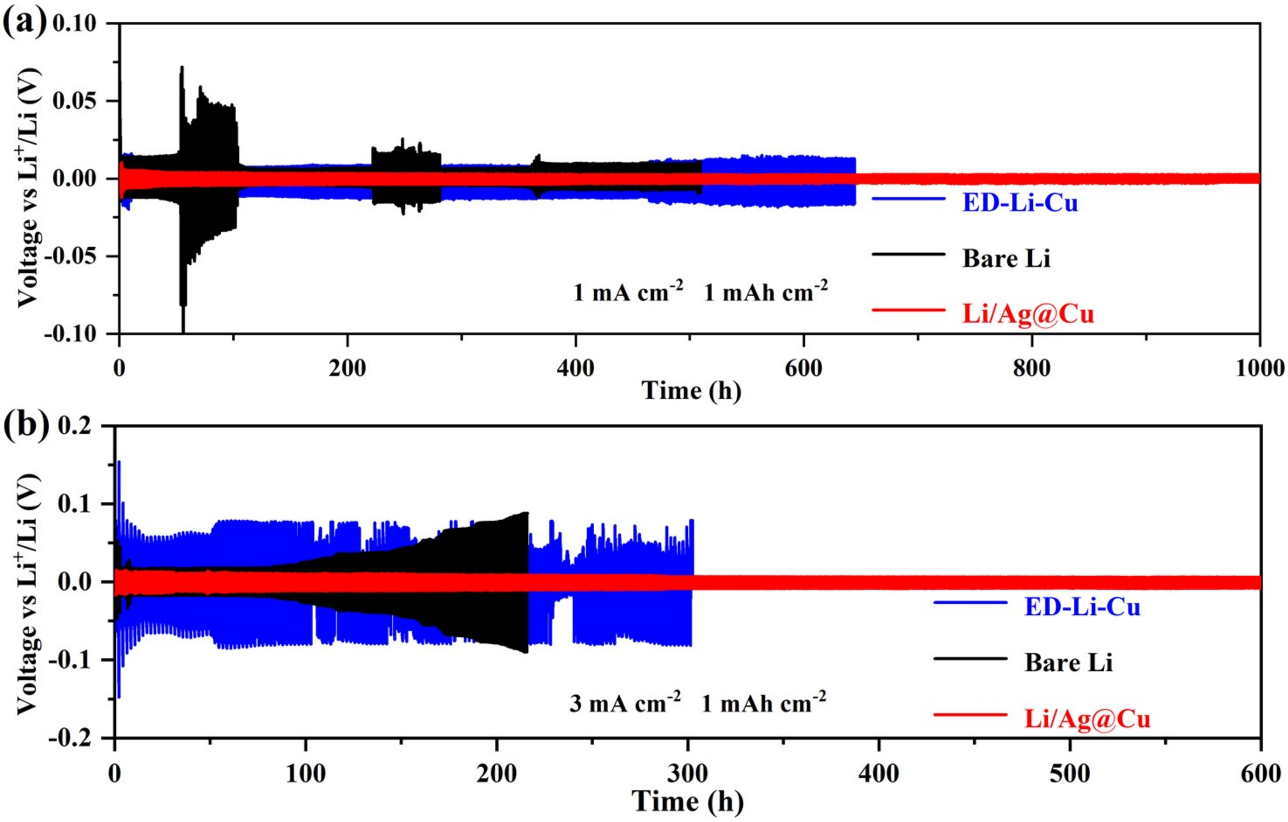

Fig. S6. Galvanostatic charge/discharge voltage profiles of the bare Li, ED-Li-Cu and Li/Ag@Cu composite electrodes in symmetric cells at the current density of (a) 1 mA cm^{-2} and (b) 3 mA cm^{-2} with the cycling capacity of 1 mAh cm^{-2}. For the further comparison of symmetrical cells, the Li composite anodes based on the Cu and Ag@Cu foam hosts should be firstly prepared. Unfortunately, the bare Cu foams without Ag modification cannot be wetted and filled by the molten Li. The molten Li impregnation method, which is facile and effective for the fabrication of the Li/Ag@Cu composite anode in our manuscript, is not suitable to prepare the metal Li and Cu composites. Therefore, the Li-Cu composite anodes are prepared by the electrochemical deposition of 10 mAh cm^{-2} Li into the bare Cu foams (denoted as ED-Li-Cu) for the symmetric cell testing. It is found that, at the current density of 1 mA cm^{-2} and cycling capacity of 1 mAh cm^{-2}, the ED-Li-Cu electrodes present an overpotential of ~20 mV during cycles, which is much higher than the Li/Ag@Cu electrodes. When the current densities increase to 3 mA cm^{-2}, the ED-Li-Cu electrodes still display higher overpotentials with irregular fluctuation. These results further confirm that the lithiophobic Cu surfaces without Ag modification bring about large barriers for electrochemical nucleation and deposition of Li, and the uncontrollable growth of Li dendrites in the large pores of Cu foams is inevitable after Li striping/plating cycles.

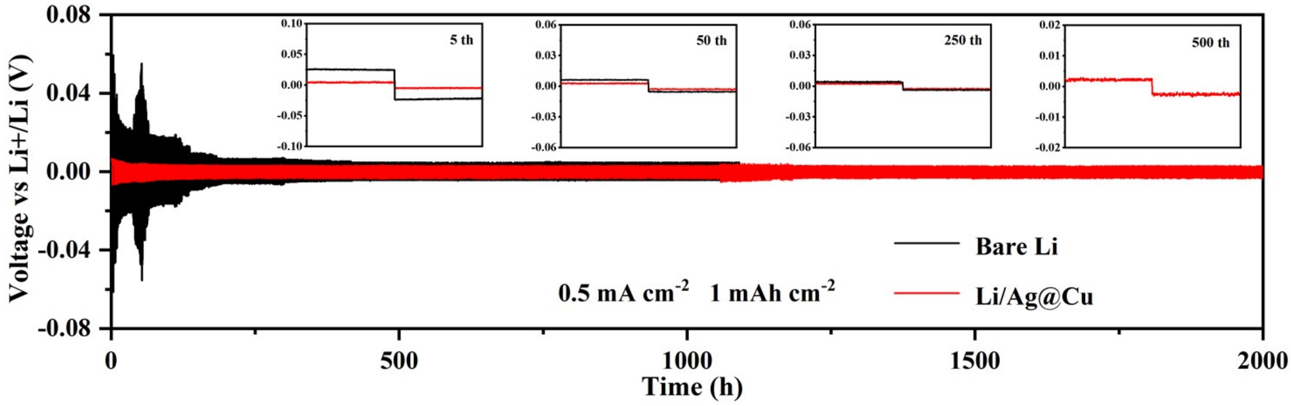

Fig. S7. Galvanostatic discharge/charge voltage profiles of the bare Li and Li/Ag@Cu composite electrodes in symmetric cells at the current density of 0.5 mA cm^{-2} and the cycling capacity of 1 mAh cm^{-2}.

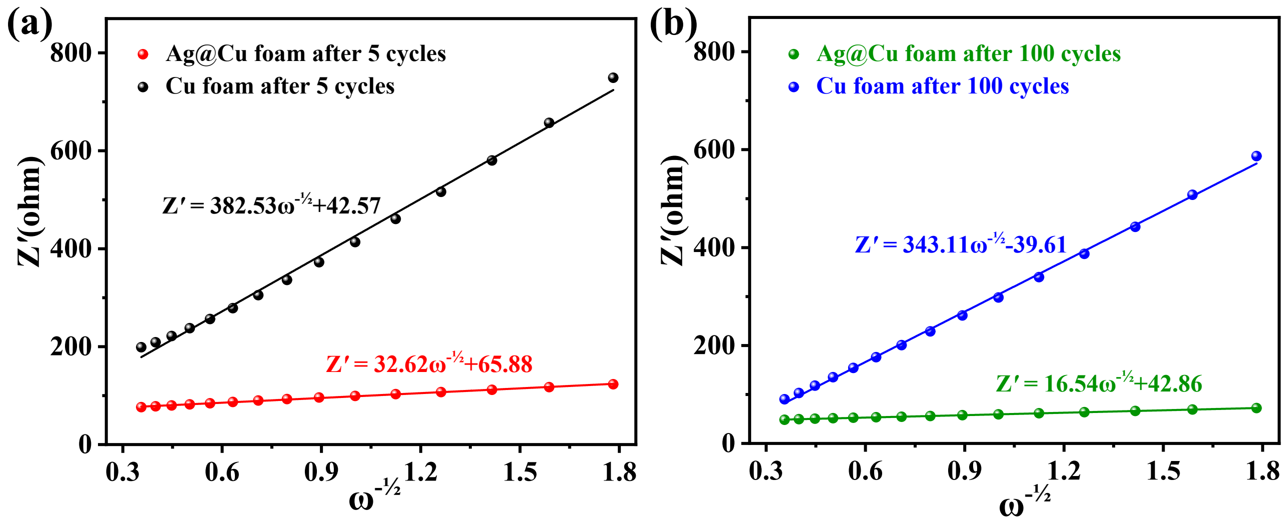

Fig. S8. Linear relationships between Z' and $\omega^{-1/2}$ from the EIS spectras of the assymmetric cells of the pristine Cu and Ag@Cu foams (a) after the 5th and (b) 100th cycles in Figure 5b. The D_{Li^+} can be calculated based on the inclined lines at the low-frequency regions of the Nyquist plots. The equation can be expressed as $D_{Li+} = \frac{R^2T^2}{2A^2n^4F^4C^2\sigma^2}$, where R is the gas constant, T is the room temperature in our experiment, A is the surface area of the electrode, n is the number of the electrons per molecule attending the electronic transfer reaction, F is the Faraday constant, C is the concentration of lithium ion in solid electrode and σ is the slope of the line Z'-$\omega^{-1/2}$. It is calculated that D_{Li^+} of the Ag@Cu foams are 1.01×10^{-10} and 3.70×10^{-10} $cm^2\ S^{-1}$ after the 5th and 100th cycles, which are much higher than those of the bare Cu foams (7.36×10^{-13} and 9.15×10^{-13} $cm^2\ S^{-1}$), indicating the enhanced Li-ion transport in the Ag@Cu foam.

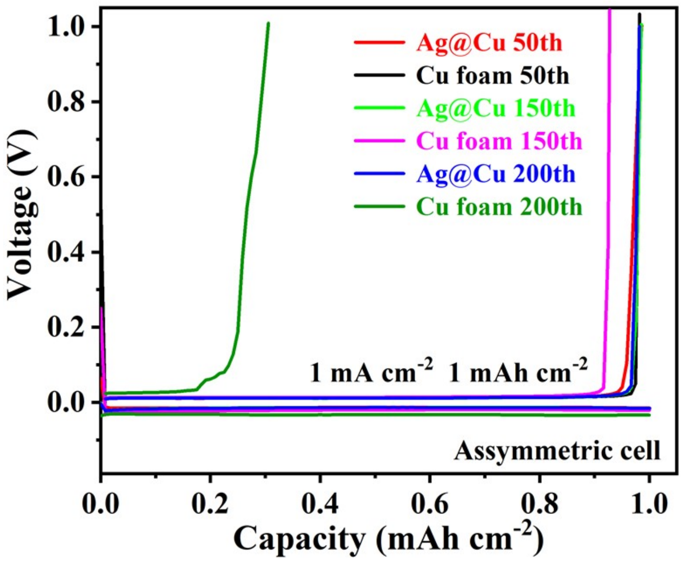

Fig. S9. Voltage-capacity profiles of the assymmetric cells of the pristine Cu and Ag@Cu foams at the current density of 1 mA cm^{-2} with the capacity of 1 mAh cm^{-2}.

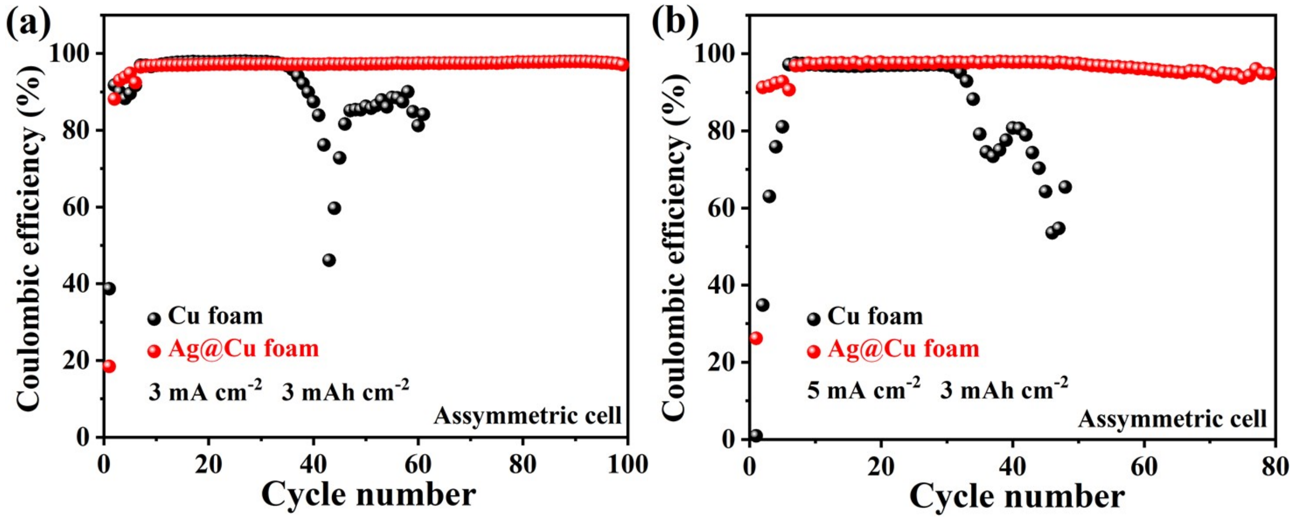

Fig. S10. The Coulombic efficiencies of the assymmetric cells of the pristine Cu and Ag@Cu foams at the current density of (a) 3 mA cm^{-2} and (b) 5 mA cm^{-2} with the Li capacity of 3 mAh cm^{-2}.

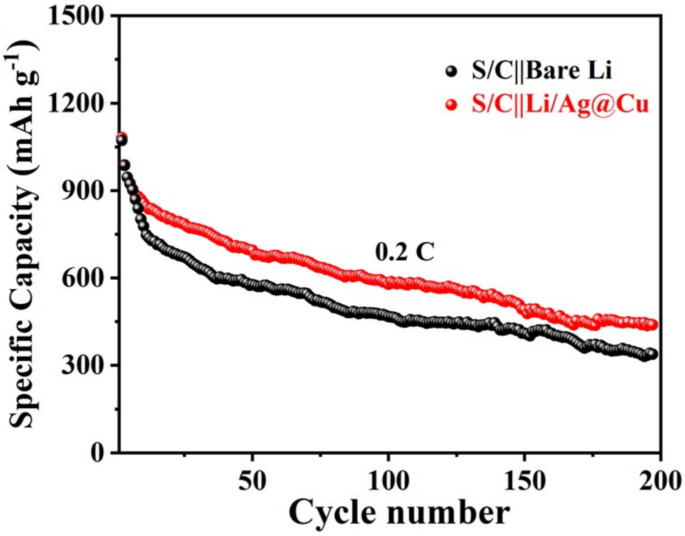

Fig. S11. Cycling performances of the S/C||Li/Ag@Cu and S/C||Li cells at 0.2 C. The mass loading of S in the cathode is ~1.1 mg cm^{-2}.

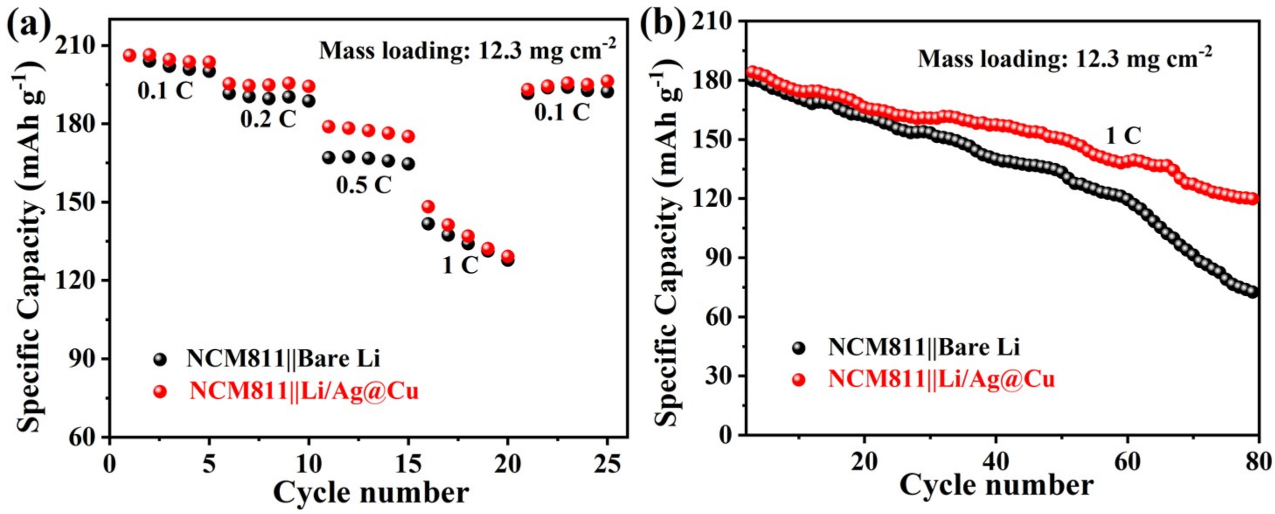

Fig. S12. (a) Rate performances and (b) cycling stabilities of the NCM811||Li/Ag@Cu and NCM811||Li cells. The mass loading of NCM811 in the cathodes is controlled to be ~12.3 mg cm^{-2}, and the N/P ratio of the NCM811 cathode to the Li/Ag@Cu anode is ~2.0.

Table S1. Comparison of the electrochemical performances of symmetric cells of Li/Ag@Cu anodes with the previously-reported Li composite anodes based on 3D hosts which are modified by the Ag nanoparticles or other lithiophilic materials in literatures.

Ref.	Li composite anodes	Lithiophilic modifers	Current densities (mA cm^{-2})	Area capacities (mAh cm^{-2})	Cycle numbers	Cycle times (h)	Stable overpotentials (mV)
S1	3D Al_2O_3/Li	Al_2O_3-based inorganic frameworks	1	1	450	900	50
			3	1	450	300	100
			8	1	240	60	400
S2	ISG-CuO/Cu foam@Li	CuO submicro-sheets	1	1	650	1300	5
			3	3	350	700	20
			5	1	300	120	450
S3	Co_3O_4/NF@Li	Co_3O_4 nanosheet arrays	1	1	225	450	25
			3	1	167	1000	40
			5	1	687	275	120
			3	3	400	800	200
S4	STM@Li	Li-Si alloy layers	2	2	400	800	50
			3	3	200	400	60
S5	3D Cu_2S NWs/Cu@Li	Cu_2S nanowires	1	1	70	140	30
S6	Li-Mn/G foam	MnO_2 nanoflake arrays	1	1	800	1600	96
			2	1	300	300	100
S7	MgO/CC@Li	MgO nanosheets	1	1	250	500	50
			3	1	90	60	155
			5	1	55	22.5	240
S8	Ni foam@Li	Ni skeletons	1	1	100	200	100
			3	1	100	67	150
			5	1	100	40	200
S9	CFC/Co-NC@Li	Co_3O_4-embedded N-doped carbon nanoflake arrays	1	1	500	1000	18
			3	1	300	200	40
			5	1	250	100	46
S10	CF/Ag-Li	Ag nanoparticles	1	1	200	400	60
			3	3	80	160	100
			10	10	30	60	120
S11	GO-Ag@Li	Ag nanoparticles	1	1	100	200	25
			2	1	150	150	140
			3	1	300	200	150
S12	Ag-NCNS@Li	Ag nanoparticles	0.5	1	500	2000	10
			1	1	930	2000	15

S13	AgNP/CNFs	Ag nanoparticles	0.5	1	125	500	20
			1	2	100	400	40
S14	CC-Ag@Li	Ag nanoparticles	1	1	375	750	25
			2	1	20	20	30
			3	1	30	20	40
			5	1	30	12	50
S15	Cu/Ag@Li	Ag nanoparticles	1	1	200	400	50
			2	2	100	200	100
S16	Cu-Ag@Li	Ag nanoparticles	0.5	1	200	800	10
			1	1	450	900	18
			3	1	750	500	35
Our work	**Li/Ag@Cu**	**Pine-needle-like Ag**	**0.5**	**1**	**500**	**2000**	**2**
			1	**1**	**500**	**1000**	**3**
			3	**1**	**900**	**600**	**6**
			5	**1**	**1500**	**600**	**8**
			3	**3**	**200**	**400**	**42**

References:

S1. L. Fan, S. Li, L. Liu, W. Zhang, L. Gao, Y. Fu, F. Chen, J. Li, H. Zhuang and Y. Lu, *Adv. Energy Mater.*, 2018, **8**, 1802350.

S2. Y. Jiang, B. Wang, A. Liu, R. Song, C. Bao, Y. Ning, F. Wang, T. Ruan, D. Wang and Y. Zhou, *Electrochim. Acta.*, 2020, **339**, 135941.

S3. G. Huang, P. Lou, G. Xu, X. Zhang, J. Liang, H. Liu, C. Liu, S. Tang, Y. Cao and S. Cheng, *J. Alloy. Compd.*, 2019, **817**, 152753.

S4. X. Yan, L. Liang, X. Han, Z. Qiao, Q. Xie, J. Lin, Z. Meng, L. Wang and D. Peng, *Chem. Eng. J.*, 2020, **373**, 1309-1318.

S5. Z. Huang, C. Zhang, W. Lv, G. Zhou, Y. Zhang, Y. Deng, H. Wu, F. Kang and Q. Yang, *J. Mater. Chem. A.*, 2018, **7**, 727-732.

S6. B. Yu, T. Tao, S. Mateti, S. Lu and Y. Chen, *Adv. Funct. Mater.*, 2018, **28**, 1803023.

S7. B. Liu, Y. Zhang, G. Pan, C. Ai, S. Deng, S. Liu, Q. Liu, X. Wang, X. Xia and J. Tu, *J. Mater. Chem. A.*, 2019, **7**, 21794-21801.

S8. S. Chi, Y. Liu, W. Song, L. Fan and Q. Zhang, *Adv. Funct. Mater.*, 2017, **27**, 1700348.

S9. G. Jiang, N. Jiang, N. Zheng, X. Chen, J. Mao, G. Ding, Y. Li, F. Sun and Y. Li, *Energy Storage Mater.*, 2019, **23**, 181-189.

S10. R. Zhang, C. Xiang, X. Shen, X. Zhang, X. Chen, X. Cheng, Y. Chong, C. Zhao and Q. Zhang, *Joule*, 2018, **2**, 764-777.

S11. H. Zhuang, P. Zhao and Y. Xu, *Inorg. Chem. Front.*, 2020, **7**, 897-904.

S12. Q. Sun, W. Zhai, G. Hou, J. Feng, L. Zhang, P. Si, S. Guo and L. Ci, *ACS Sustain. Chem. Eng.*, 2018, **6**, 15219-15227.

S13. C. Yang, Y. Yao, S. He, H. Xie, E. Hitz and L. Hu, *Adv. Mater.*, 2017, **29**, 1702714.

S14. C. Hao, H. Jin, H. Liu, N. Cai, C. Gao, P. Zhang and M. Wang, *J. Electroanal. Chem.*, 2020, **878**, 114569.

S15. Z. Hou, Y. Yu, W. Wang, X. Zhao, Q. Di, Q. Chen, W. Chen, Y. Liu and Z. Quan, *ACS Appl. Mater. Inter.*, 2019, **11**, 8148-8154.

S16. S. Cui, P. Zhai, W. Yang, Y. Wei, J. Xiao, L. Deng and Y. Gong, *Small*, 2020, **16**, 1905620.